Research Article | Vol. 27, No. 21 | 14 Oct 2019 | OPTICS EXPRESS 30441
Optics EXPRESS

Time-division-multiplexed observation bandwidth for ultrafast parametric spectro-temporal analyzer

NINGNING YANG,[1] LIAO CHEN,[1] LUN LI,[1] YAOSHUAI LI,[1] CHI ZHANG,[1,3] YI WANG,[1,4] KENNETH K. Y. WONG,[2] AND XINLIANG ZHANG[1]

[1]*Wuhan National Laboratory for Optoelectronics, Huazhong University of Science and Technology, Wuhan 430074, China*
[2]*Photonics Systems Research Laboratory, Department of Electrical and Electronics Engineering, The University of Hong Kong, Pokfulam Road, Hong Kong, China*
[3]*chizheung@hust.edu.cn*
[4]*ywangwnlo@hust.edu.cn*

Abstract: Parametric spectro-temporal analyzer (PASTA) has been demonstrated as a powerful tool for ultrafast spectrum measurement with superior frame rate and resolution. Compared with other time-stretch-based counterparts, the temporal focusing mechanism enlarges the initial condition and enables the observation of arbitrary waveform, especially the emission spectrum. However, due to the limited conversion bandwidth of the parametric mixing–based time-lens, the observation bandwidth of PASTA is constrained within the C (conventional) band, which hinders its practical applications. To overcome this constraint, both stokes and anti-stokes conversions of the parametric mixing process are leveraged, and the concept of time division multiplexing (TDM) is introduced to ensure their separability. Therefore, the TDM-based PASTA system successfully demultiplexes the C band and L (long) band spectra in two adjacent temporal frames. It is capable of reconstructing the wavelength-to-time sequence for arbitrary waveform over a record 58-nm observation bandwidth, which can be further improved by optimizing the filters and amplifiers. Meanwhile, both of these two bands achieve 20-pm resolution, 10-MHz frame rate, and –30-dBm sensitivity. Moreover, this TDM concept can also be applied to other parametric mixing–based temporal imaging systems to enlarge the working wavelength band, such as temporal magnification.

1. Introduction

With the rapidly increasing of communication capacity, the research on ultrafast phenomenon is getting more and more attention [1–4]. Among numerous research methods, real-time optical spectrum analysis occupies an indispensable position. However, the most conventional optical spectrum analyzer (OSA) is based on the monochromator. Its mechanical scanning process limits the frame rate (~5 Hz) and cannot capture some spectral dynamics, such as the state evolution of a laser cavity, real-time chemical or physical reaction, etc [5,6]. Polychromator based on the charge-coupled device (CCD) sensor enables faster operation (usually less than 1 kHz), but significantly compromises its accuracy [7]. Alternatively, dispersive Fourier transformation (DFT) technology has been introduced and demonstrated in many ultrafast applications [8–11]. Leveraging the large bandwidth of the single-pixel detector, the DFT based spectroscopy achieves MHz range frame rate, and has played an important role in studying some non-repetitive and statistically rare phenomena that occur on short timescales [12,13]. Nevertheless, some constraints still exist. First, its input condition is confined to short pulses, which makes it usually operate as an absorption spectroscopy [14]. Second, despite the loss along the dispersive medium can be compensated by amplification

#377087 https://doi.org/10.1364/OE.27.030441
Journal © 2019 Received 5 Sep 2019; revised 21 Sep 2019; accepted 23 Sep 2019; published 7 Oct 2019

Optics EXPRESS

technology, the pulse stretching is essentially an energy diverging process which inevitably degrades the detection sensitivity [9].

In view of these constraints, a time lens focusing mechanism based parametric spectro-temporal analyzer (PASTA) was introduced, and its initial condition can be greatly enlarged [15]. In other words, it can reconstruct the wavelength-to-time sequence for arbitrary waveform. Moreover, compared with the DFT technology, it can achieve higher spectral resolution under the same amount of output dispersion. Previous PASTA system has achieved 20-pm spectral resolution and –40-dBm detection sensitivity, under 100-MHz frame rate [16,17]. The spectral resolution can be further improved with a large temporal numerical aperture time lens enabled by a dispersion-engineered silicon waveguide or introduction of the heterodyne technique [18,19]. While its drawbacks are also obvious, it can only observe 30-nm wavelength range in C-band [20], which is mainly limited by the conversion bandwidth of the parametric mixing and the amplification window. Nevertheless, as the rapid growth of communication capacity, advanced modulation formats are applied and the spectral efficiency is close to the so-called nonlinear Shannon limit [21–25]. Further capacity increase can be realized by extending the wavelength range beyond conventional C band (range from 1530 to 1570 nm) [26]. Large-capacity systems in L band (range from 1570 to 1610 nm) are already commercial available [27–29]. As a result, the corresponding fields also need coordinated development, so as to the real-time optical spectrum analysis [30–32]. It is highly desired that, real-time optical spectrum analysis configuration can cover both C-band and L-band. To extend the observation bandwidth to the L-band range, it is possible to simply reverse the direction of the parametric mixing process, with almost identical system configuration. However, these two schemes cannot simply combine together to observe both C-band and L-band, because the bidirectional parametric mixing process would make the newly generated idler merge together with the original signal, and cannot fully separate with each other.

In this study, the C-band PASTA and L-band PASTA are combined together through the time-division multiplexing (TDM) technology, and successfully overcome the aforementioned overlapping issue. The TDM based PASTA system covers the observation bandwidth of both C-band and L-band, and the total observation wavelength range is up to 58 nm, ranging from 1527.8 to 1554.8 nm and 1566.8 to 1597.8 nm. It also achieves 20-pm spectral resolution and –30-dBm detection sensitivity under 10-MHz frame rate. For this purpose, the TDM based PASTA system enhances the ability of observing the spectrum of some dynamic phenomena and non-repetitive events, and instructs the theoretical analysis and practical application. Moreover, this TDM based technique can be applied to other similar parametric mixing systems for expanding conversion wavelength band, such as temporal magnification and real-time full-field measurement [33,34].

2. Principle

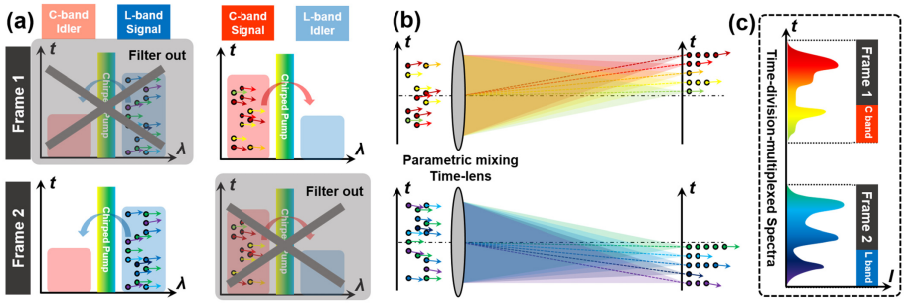

Fig. 1. Schematic of the TDM based PASTA system. (a) Parametric mixing based time-lens in two temporal adjacent frames, with interleaved wavelength relation. (b) Temporal ray diagram of the TDM based PASTA system [16]. The vertical axis refers to time, the horizontal axis refers to dispersion, and the axial angle refers to different frequencies. (c) Time-division-multiplexed spectra of two wavelength bands.

Optics EXPRESS

Schematic of the TDM based PASTA is shown in Fig. 1. According to Fourier optics, the spatial frequency spectrum of the incident light can be obtained at the focal plane of a converging lens, which is described as the spatial Fourier transform process. The PASTA system is the time domain counterpart based on the space-time duality. Different optical frequency components will focus on different temporal positions at the focal time axis, resulting in wavelength-to-time mapping. Here, the input signal is described as $E_0(t)$, and an ideal time lens is realized by temporal quadratic phase modulation, with the transfer function of $t_f(t) = \exp(-it^2/4\Phi_f)$, where Φ_f is the focal group delay dispersion (GDD). As the frequency chirp is obtained from the differential of the phase term of $t_f(t)$, the converged optical field becomes a linear swept-source when $E_0(t)$ is a continuous-wave (CW) source. Then, the swept-source will be focused by a dispersive fiber, which adds a quadratic phase modulation in the frequency domain: $G_o(\omega) = \exp(-i\Phi_o\,\omega^2/2)$, with the output GDD $\Phi_o = \Phi_f$. Detailed derivation can be found in our previous work [15], and the focused optical field $E_1(t)$ can be expressed as:

$$E_1(t) = \frac{1}{\sqrt{2\pi i\Phi_f}} \exp\left(i\frac{t^2}{2\Phi_f}\right) \bar{E}_0\left(\frac{t}{\Phi_f}\right), \tag{1}$$

where $\bar{E}_0(\omega)$ is the Fourier transform of the input optical field $E_0(t)$. From Eq. (1), it is easy to find that the output optical filed is the Fourier transform of input signal, and the extra phase item can be ignored after the square law detector. The wavelength-to-time mapping relation can also be obtained:

$$\Delta t = \frac{2\pi c\Phi_f}{\lambda_0^2}\Delta\lambda. \tag{2}$$

It describes the basic function of PASTA, which maps the spectra information into temporal domain and enables the real-time spectrum analysis. However, limited by the FWM conversion bandwidth and amplification bandwidth, the original PASTA can only operate in C band. To enlarge the observation bandwidth within the amplification bandwidth, the two conversion bands of the FWM process attract our attention, and it corresponds to the C-band and L-band, respectively. However, if the signal of both C-band and L-band are launched into the PASTA system simultaneously, as shown in Fig. 1(a), their newly generated idlers and original signal will overlapped with each other, and cannot be separated in the output time axis. To circumvent this problem, the TDM technology is introduced here: in two temporal adjacent frames, only single band is remained within each frame; therefore, different wavelength bands are observed in difference temporal windows, as shown in Figs. 1(b) and 1(c). It is noted that, the observation bandwidth is almost doubled in this scheme, from 30 to 58 nm, without introducing any tailor-made amplifiers or parametric mixing medium. Although the frame rate of this spectroscopy is halved accordingly, the enlarged observation bandwidth will definitely enable more applications.

3. Experimental results and discussion

Figure 2 gives the detailed signal flow graph of the proposed TDM based PASTA. The signal under test contains both C-band and L-band, which are first separated into two channels by a wavelength splitter, as shown in Fig. 2(b). To prevent the mixing with the newly generated idlers, the TDM is applied here, and includes two steps: the pulse picking Fig. 2(c) and the wavelength dependent time delay Fig. 2(d) by a frame period ($\Delta\tau$ = 50 ns, corresponds to the frame rate of 20 MHz). Then, the wideband signal in the TDM format is prepared for the conventional PASTA measurement, and the parametric mixing based time-lens is performed in Fig. 2(e). Here, the 1-nm chirped pump centered at 1561.5 nm is stretched by a spool of single mode fiber with a GDD of $2\Phi_f$ (Φ_f = –1791.6 ps^2), and it is acted as the pump of the

Optics EXPRESS

parametric mixing process. To remove the original signal and remain the newly generated idlers, temporal delay based pulse picking is applied in Figs. 2(f)–2(h). Therefore, the temporal focusing process can be simply performed by passing through a spool of dispersion compensation fiber (DCF) with the GDD of $-\Phi_f$ and compensated third-order dispersion, as shown in Fig. 2(i). Finally, it is detected and acquired by a 40-GHz photodetector and a 33-GHz oscilloscope, and the spectra of C-band and L-band are displayed in the neighboring temporal frames in Fig. 2(j).

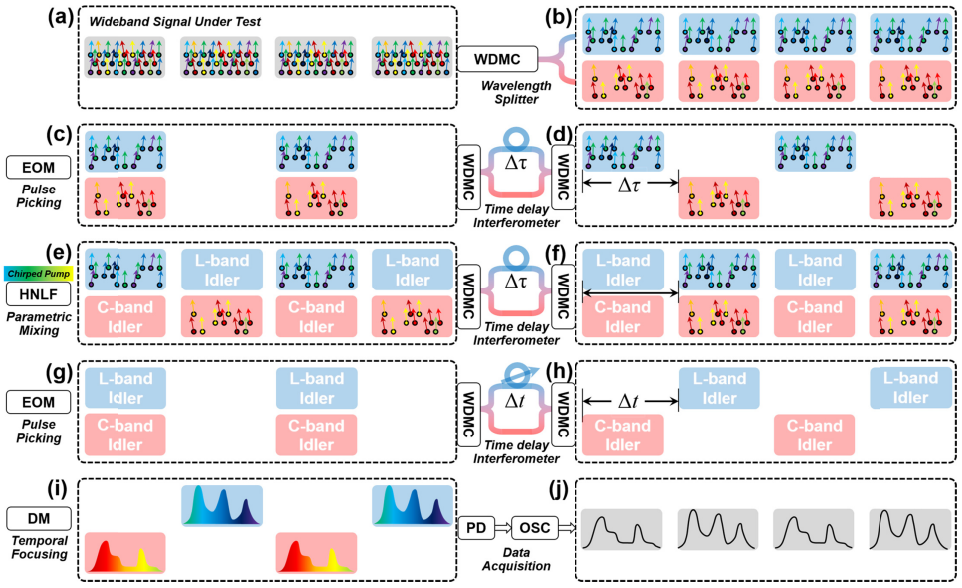

Fig. 2. Detailed signal flow graph of the TDM based PASTA with extended observation bandwidth. WDMC: wavelength division multiplexing coupler; EOM: electro-optic modulator; HNLF: highly nonlinear fiber; DCF: dispersion compensation fiber; PD: Photodetector; OSC: Oscilloscope.

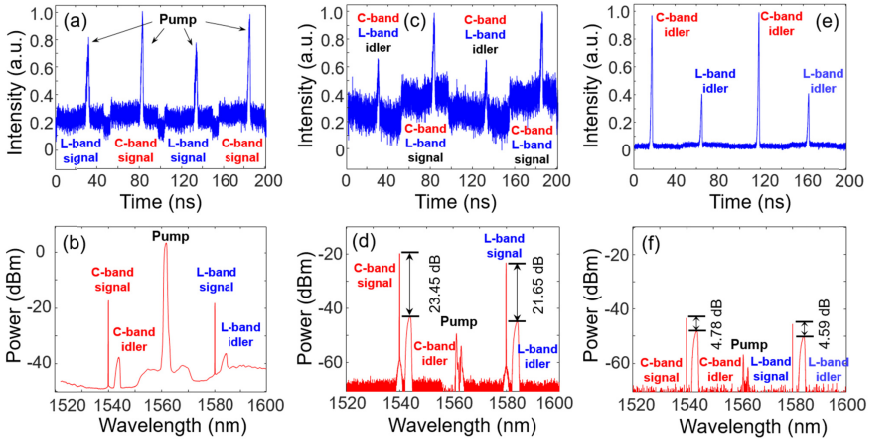

Fig. 3. Temporal waveforms and spectra of the intermediate processes of the TDM based PASTA, with two CW signals at 1540 nm (C-band) and 1580 nm (L-Band). (a) & (b) After parametric mixing, corresponds to Fig. 2(e); (c) & (d) before the second pulse picking, corresponds to Fig. 2(f); (e) & (f) before the temporal focusing, corresponds to Fig. 2(h), where the temporal profile (e) is amplified to enhance the signal-to-noise ratio.

Optics EXPRESS

Figure 3 shows some intermediate processes of the TDM based PASTA, which are essential to monitor the criteria of the TDM technology. To explore its extended bandwidth in both C-band and L-band, two CW signals at 1540 and 1580 nm are launched into the system simultaneously. After separate them in the temporal domain, they have the parametric mixing with the chirped pump, and the newly generated idler spectrum is shown in Fig. 3(b); while in the temporal domain, the idler is overlapped with the pump pulse (Fig. 3(a)). Therefore, by filtering out the pump and channelized temporal delay, the idlers are overlapped in the temporal domain, as shown in Figs. 3(c) and 3(d). But it is obvious that there is still a high pulse upon the CW signal in Fig. 3(c), which are induced by XGM between the CW signals and pump pulse and have also been seen in theoretical simulation. Afterwards, an EOM with 20-dB extinction ratio is applied to eliminate the original CW signal components, and it is observed from Figs. 3(d) and 3(f) that the CW components are compressed by ~18 dB. In the temporal domain, only the idlers exist in Fig. 3(e). It should be note that, the inconsistency in intensity between Figs. 3(e) and 3(f) is due to the spectrum Fig. 3(f) being obtained directly after the EOM, and the temporal waveform Fig. 3(e) is amplified to enhance the signal-to-noise ratio.

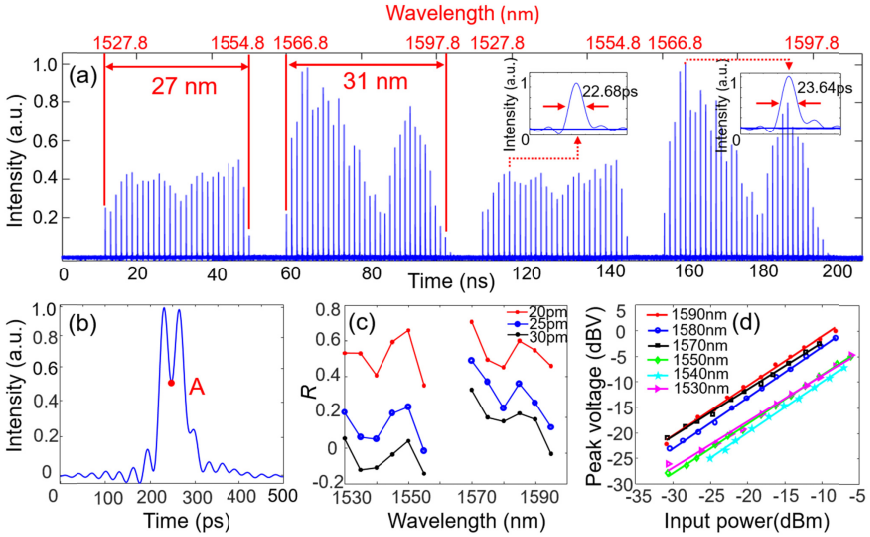

Fig. 4. Characterization of the PASTA system with extended observation bandwidth. (a) Observation bandwidth performance in four frame periods. (b) Resolution performance of two CW components separated by 20 pm. (c) Resolving power versus different wavelength spacing. (d) Dynamic range response over different wavelengths.

To characterize the PASTA system with extended observation bandwidth, its wavelength range, resolution, and dynamic range are explored here. First, the CW signals are spanning from 1527.8 to 1554.8 nm and 1566.8 to 1598.8 nm, which corresponds to the extended observation bandwidth of ~60 nm, as shown in Fig. 4(a). The intensity fluctuation is due to the wavelength dependent amplification in this system, though it can be easily calibrated by removing the envelop. Second, for each single CW component, its full-width at half-maximum (FWHM) pulsewidth is 23 ps, which responses to 16.2 pm spectral width. More specific, the resolution is quantified by resolving two adjacent CW sources, as shown in Fig. 4(b), where the two CW components spaced by 20 pm are just separated at its half maximum. Here a parameter, R corresponds to the normalized intensity of point A, is introduced to represent the resolving power, the smaller the better. It can be concluded from Fig. 4(c) that the spectral resolution across the observation range is around 20 pm, and its fluctuation is due to the existence of higher-order dispersion in the output dispersion. Figure 4(d) gives the

Optics EXPRESS

response curve between output pulse peak voltage and input CW power. The sensitivity is around –30 dBm and the response characteristics are almost linear over 25 dB dynamic range.

Finally, the wideband spectrum analysis is investigated by comparing the TDM based PASTA with a conventional OSA, as depicted in Fig. 5. Compared with the ADFT technology, one of the key advantages of the PASTA is the large temporal observation window based on the temporal focusing mechanism, and arbitrary waveform can be measured accordingly, including the noise source. Thus the spectrum under test is comprised by two CW components separated by 20 pm, and a wideband amplified spontaneous emission (ASE) noise source filtered by equally spaced comb filter. Figures 5(a) and 5(d) show the non-average spectra of C-band and L-band signals obtained by the TDM based PASTA, respectively. The averaging process will make the spectra smoother as shown in Figs. 5(b) and 5(e), though the frame rate also decreases. The difference between Figs. 5(a) and 5(b), Figs. 5(d) and 5(e) reveals that the randomness of the noise source would result in the fluctuation of instantaneous spectrum, though it is statistically flat under the long accumulation time. As a comparison, the measurement by a conventional OSA with 10-pm resolution is shown in Figs. 5(c) and 5(f), with frame rate in several hertz range. In general, these results manifest the TDM based PASTA is capable of capturing spectral information in arbitrary waveforms, and its resolution performance is comparable to the state-of-art OSA.

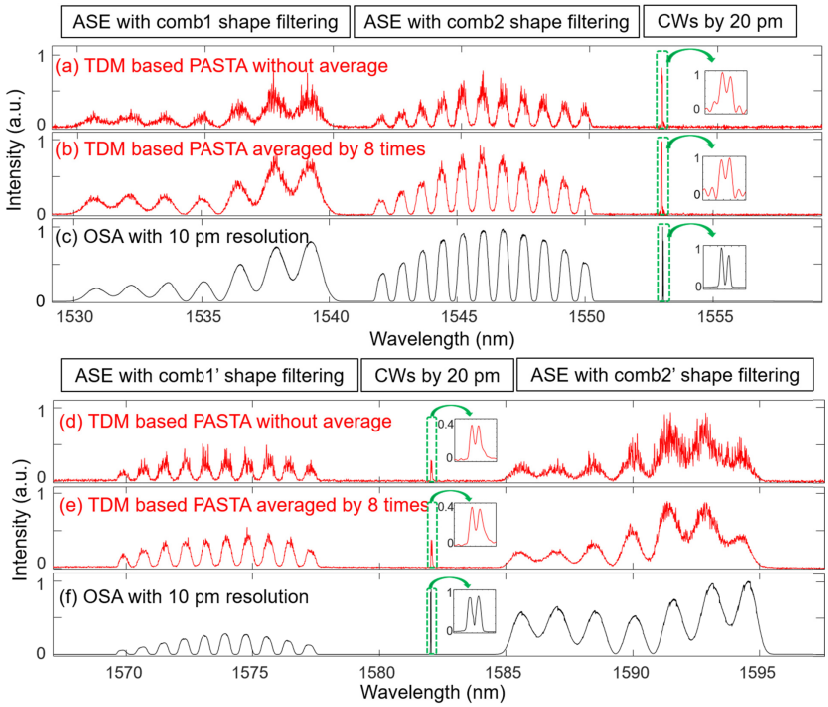

Fig. 5. Wideband spectrum analysis performance the TDM based PASTA, compared with a conventional OSA. (a) & (d) Spectra obtained by the TDM based PASTA without average; (b) & (e) averaged by 8 times; (c) & (f) Spectra obtained by OSA with a 10-pm resolution.

4. Conclusions

To sum up, a TDM based PASTA with extended observation bandwidth has been proposed and experimentally demonstrated. Due to its fast frame rate and high resolution, the PASTA system based on temporal focusing mechanism has drawn more and more attention. However, its observation bandwidth is limited by the parametric mixing based time-lens, and only unidirectional conversion is performed to avoid overlapping between both conversion

Optics EXPRESS

bandwidth. To overcome this constraint, in this paper, the TDM technology is introduced, which enables bidirectional conversion of the parametric mixing process, and the signal from C-band and L-band will be observed in time sequence. As a result, the TDM based PASTA extended the observation bandwidth to 58 nm, ranging from 1527.8 to 1554.8 nm and 1566.8 to 1597.8 nm. It can be further improved with larger bandwidth amplifiers and more suitable filters. In addition, it has a spectral resolution of 20 pm, a sensitivity of –30 dBm (1 μW), and a frame rate of 10 MHz. It is believed that this TDM based PASTA is promising for a wider applications in ultrafast spectroscopy.

Funding

National Natural Science Foundation of China (61927817, 61735006, 61675081, 61505060, 61320106016); NSFC/RGC Joint Research Scheme (61631166003, N_HKU712/16); China Postdoctoral Science Foundation (2018M640692).

Disclosures

The authors declare no conflicts of interest.

References

1. Y. Pu, W. Wang, R. B. Dorshow, B. B. Das, and R. R. Alfano, "Review of ultrafast fluorescence polarization spectroscopy [invited]," Appl. Opt. **52**(5), 917–929 (2013).
2. M. Liu, A. P. Luo, Y. R. Yan, S. Hu, Y. C. Liu, H. Cui, Z. C. Luo, and W. C. Xu, "Successive soliton explosions in an ultrafast fiber laser," Opt. Lett. **41**(6), 1181–1184 (2016).
3. H. Hou, B. Yang, X. Mao, V. Zorba, P. Ran, and R. E. Russo, "Characteristics of plasma plume in ultrafast laser ablation with a weakly ionized air channel," Opt. Express **26**(10), 13425–13435 (2018).
4. Q. Guo, R. Yu, C. Li, S. Yuan, B. Deng, F. J. García de Abajo, and F. Xia, "Efficient electrical detection of mid-infrared graphene plasmons at room temperature," Nat. Mater. **17**(11), 986–992 (2018).
5. A. B. Shafer, L. R. Megill, and L. A. Droppleman, "Optimization of the Czerny–Turner spectrometer," J. Opt. Soc. Am. **54**(7), 879–887 (1964).
6. O. Svelto, *Principles of Lasers*, 4th ed. (Plenum University 1998).
7. T. G. Etoh, C. V. Le, Y. Hashishin, N. Otsuka, K. Takehara, H. Ohtake, T. Hayashida, and H. Maruya, "Evolution of Ultra-High-Speed CCD Imagers," Plasma Fusion Res. **2**, S1021 (2007).
8. D. R. Solli, J. Chou, and B. Jalali, "Amplified wavelength-time transformation for real-time spectroscopy," Nat. Photonics **2**(1), 48–51 (2008).
9. K. Goda and B. Jalali, "Dispersive Fourier transformation for fast continuous single-shot measurements," Nat. Photonics **7**(2), 102–112 (2013).
10. J. Azana and M. A. Muriel, "Real-Time Optical Spectrum Analysis Based on the Time–Space Duality in Chirped Fiber Gratings," IEEE J. Quantum Electron. **36**(5), 517–526 (2000).
11. G. Herink, B. Jalali, C. Ropers, and D. R. Solli, "Resolving the build-up of femtosecond mode-locking with single-shot spectroscopy at 90 MHz frame rate," Nat. Photonics **10**(5), 321–326 (2016).
12. M. Liu, A. P. Luo, Y. R. Yan, S. Hu, Y. C. Liu, H. Cui, Z. C. Luo, and W. C. Xu, "Successive soliton explosions in an ultrafast fiber laser," Opt. Lett. **41**(6), 1181–1184 (2016).
13. G. Herink, F. Kurtz, B. Jalali, D. R. Solli, and C. Ropers, "Real-time spectral interferometry probes the internal dynamics of femtosecond soliton molecules," Science **356**(6333), 50–54 (2017).
14. J. Chou, Y. Han, and B. Jalali, "Time-wavelength spectroscopy for chemical sensing," IEEE Photonics Technol. Lett. **16**(4), 1140–1142 (2004).
15. C. Zhang, X. Wei, and K. K. Y. Wong, "Performance of parametric spectro-temporal analyzer (PASTA)," Opt. Express **21**(26), 32111–32122 (2013).
16. C. Zhang, J. Xu, P. C. Chui, and K. K. Y. Wong, "Parametric spectro-temporal analyzer (PASTA) for real-time optical spectrum observation," Sci. Rep. **3**(1), 2064 (2013).
17. H. Zhou, L. Chen, X. Zhou, C. Zhang, K. K. Y. Wong, and X. Zhang, "Temporal stability and spectral accuracy enhancement of the spectro-temporal analyzer," IEEE Photonics Technol. Lett. **29**(22), 1971–1974 (2017).
18. H. Zhou, N. Yang, G. Liu, L. Chen, Y. Wang, C. Zhang, K. K. Y. Wong, and X. Zhang, "Large-Temporal-Numerical-Aperture Parametric Spectro-Temporal Analyzer Based on Silicon Waveguide," IEEE Photonics J. **11**(5), 7102710 (2019).
19. A. Tikan, S. Bielawski, C. Szwaj, S. Randoux, and P. Suret, "Single-shot measurement of phase and amplitude by using heterodyne time-lens and ultrafast digital time-holography," Nat. Photonics **12**(4), 228–234 (2018).
20. B. Li, Y. Wei, J. Kang, C. Zhang, and K. K. Y. Wong, "Parametric spectrotemporal analyzer based on four-wave mixing Bragg scattering," Opt. Lett. **43**(8), 1922–1925 (2018).
21. M. S. Faruk and S. J. Savory, "Digital signal processing for coherent transceivers employing multilevel formats," J. Lightwave Technol. **35**(5), 1125–1141 (2017).

Optics EXPRESS

22. A. Muhammad, G. Zervas, and R. Forchheimer, "Resource allocation for space-division multiplexing: Optical white box versus optical black box networking," J. Lightwave Technol. **33**(23), 4928–4941 (2015).
23. Z. Ghaseemlooy, W. O. Popoola, and S. Rajbhandri, *Optical Wireless Communications, System and Channel Modelling With Matlab* (CRC University, 2012).
24. P. J. Winzer, "High-spectral-efficiency optical modulation formats," J. Lightwave Technol. **30**(24), 3824–3835 (2012).
25. A. D. Ellis, J. Zhao, and D. Cotter, "Approaching the non-linear Shannon limit," J. Lightwave Technol. **28**(4), 423–433 (2010).
26. S. Bindhaiq, A. S. M. Supa'at, N. Zulkifli, A. B. Mohammad, R. Q. Shaddad, M. A. Elmagzoub, and A. Faisal, "Recent development on time and wavelength-division multiplexed passive optical network (TWDM-PON) for next-generation passive optical network stage 2 (NG-PON2)," J. Opt. Switch Network **15**, 53–66 (2015).
27. E. Agrell, M. Karlsson, A. R. Chraplyvy, D. J. Richardson, P. M. Krummrich, P. Winzer, K. Roberts, J. K. Fisher, S. J. Savory, B. J. Eggleton, M. Secondini, F. R. Kschischang, A. Lord, J. Prat, I. Tomkos, J. E. Bowers, S. Srinivasan, M. B. Pearce, and N. Gisin, "Roadmap of optical communications," J. Opt. **18**(6), 063002 (2016).
28. P. Marin-Palomo, J. N. Kemal, M. Karpov, A. Kordts, J. Pfeifle, M. H. P. Pfeiffer, P. Trocha, S. Wolf, V. Brasch, M. H. Anderson, R. Rosenberger, K. Vijayan, W. Freude, T. J. Kippenberg, and C. Koos, "Microresonator-based solitons for massively parallel coherent optical communications," Nature **546**(7657), 274–279 (2017).
29. A. Sano, T. Kobayashi, S. Yamanaka, A. Matsuura, H. Kawakami, Y. Miyamoto, K. Ishihara, and H. Masuda, "102.3-Tb/s (224 × 548-Gb/s) C- and extended L-band all-Raman transmission over 240 km using PDM-64QAM single carrier FDM with digital pilot tone," in *Proceedings of Optical Fiber Communication Conference* (OFC/NFOEC, 2012), paper PDP5C.3.
30. B. Stern, X. Ji, Y. Okawachi, A. L. Gaeta, and M. Lipson, "Battery-operated integrated frequency comb generator," Nature **562**(7727), 401–405 (2018).
31. M. A. Foster, A. C. Turner, J. E. Sharping, B. S. Schmidt, M. Lipson, and A. L. Gaeta, "Broad-band optical parametric gain on a silicon photonic chip," Nature **441**(7096), 960–963 (2006).
32. K. J. A. Ooi, D. K. T. Ng, T. Wang, A. K. L. Chee, S. K. Ng, Q. Wang, L. K. Ang, A. M. Agarwal, L. C. Kimerling, and D. T. H. Tan, "Pushing the limits of CMOS optical parametric amplifiers with USRN:Si_7N_3 above the two-photon absorption edge," Nat. Commun. **8**(1), 13878 (2017).
33. A. Klein, G. Masri, H. Duadi, K. Sulimany, O. Lib, H. Steinberg, S. A. Kolpakov, and M. Fridman, "Ultrafast rogue wave patterns in fiber lasers," Optica **5**(7), 774–778 (2018).
34. P. Ryczkowski, M. Närhi, C. Billet, J.-M. Merolla, G. Genty, and J. M. Dudley, "Real-time full-field characterization of transient dissipative soliton dynamics in a mode-locked laser," Nat. Photonics **12**(4), 221–227 (2018).